

Supporting Information for: Development and Characterization of
Ultrafiltration TiO₂ Magnéli Phase Reactive Electrochemical
Membranes

*Lun Guo, Yin Jing, and Brian P. Chaplin**

Department of Chemical Engineering, University of Illinois at Chicago, 810 S. Clinton St.,
Chicago, IL 60607, USA

*Corresponding author: phone: 217-369-5529; fax: 312-996-0808; e-mail: chaplin@uic.edu

Prepared January 14, 2016

For:

Environmental Science and Technology

12- Pages

8- Figures

1- Tables

1) Materials and Methods

Cross-flow Filtration Setup. The REM was used as working electrode, and a 1.6 mm diameter 316 stainless steel rod was used as counter electrode. A leak-free Ag/AgCl reference electrode (Warner Instruments, LF-100) was placed ~ 0.85 mm from the inner REM surface. Potentials were applied and monitored using a Gamry Reference 600 potentialstat/galvanostat. For EIS measurements, a silver wire was used as a pseudo reference electrode, due to the high impedance of the Ag/AgCl reference. All potentials were corrected for solution resistance, which was calculated by EIS measurements, and potentials are reported versus the standard hydrogen electrode (SHE). Reynolds numbers for membrane cross-flow ranged between 312 and 1247 (laminar).

Reaction Rate Characterization. Experiments were conducted with a solution of 5 mM Fe(CN)_6^{4-} and 5 mM Fe(CN)_6^{3-} in a 100 mM KH_2PO_4 supporting electrolyte, and I_{lim} was determined by scanning the anodic potential at $v = 100 \text{ mV s}^{-1}$, starting at the OCP. The permeate flux (J) was controlled by varying ΔP (0 to 103 kPa). An additional measurement of I_{lim} at REM-3 was performed at a $v = 10 \text{ mV s}^{-1}$ and in an electrolyte consisting of 5 mM Fe(CN)_6^{4-} , 20 mM Fe(CN)_6^{3-} , and 100 mM KH_2PO_4 in order to insure that neither cathodic reactions nor non-faradaic current interfered with I_{lim} measurements. The REM was initially operated with a permeate flux of 800 LMH, where both feed and permeate solutions were recycled for 30 min. After which, LSV was performed at $J = 110$ to 950 LMH, in order to assess the effect of J on k_{obs} .

2) Hg Porosimetry

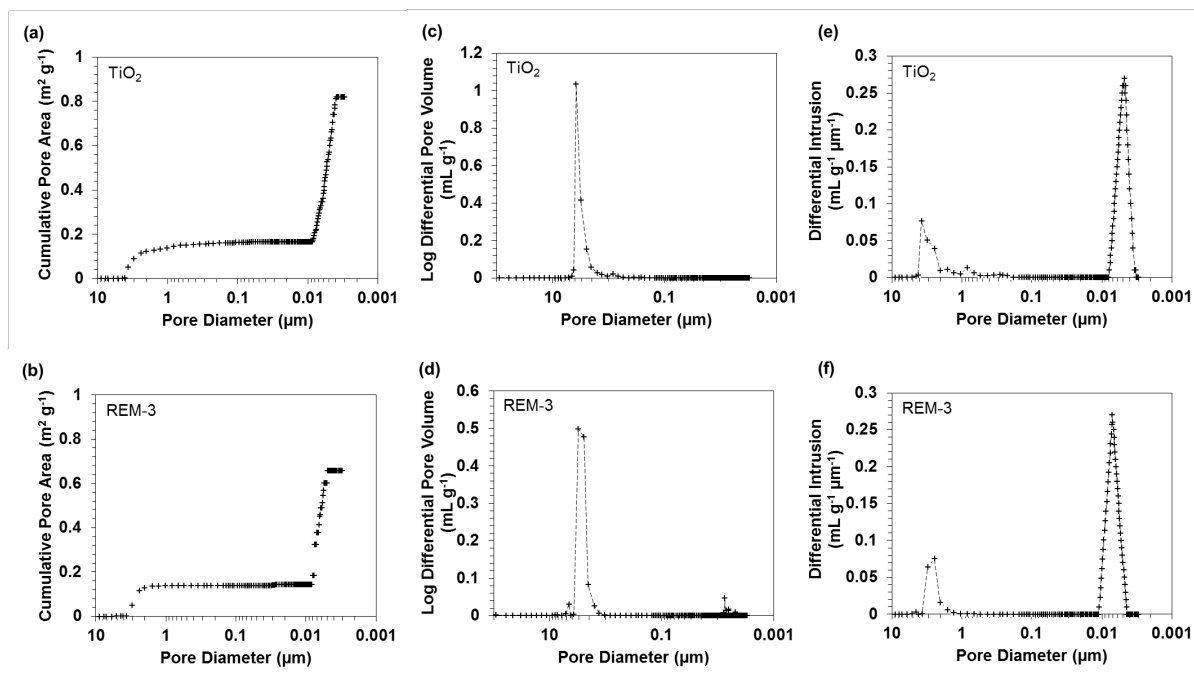


Figure S-1. Hg porosimetry analysis of cumulative pore area for (a) precursor TiO_2 membrane (b) REM-3, log differential pore volume data for (c) precursor TiO_2 membrane and (d) REM-3, and differential intrusion for (e) precursor TiO_2 and (f) REM-3.

3) Molecular weight cut-off (MWCO) Determination.

All MWCO experiments on the pristine TiO₂ membrane and REM-3 were performed in the cross-filtration setup in a dead-end filtration mode. Prior to a MWCO experiment, DI water was circulated in the system until steady state, and permeate flux J_0 was used to indicate the state of the membrane. The feed was replaced with a dextran solution of a given molecular weight, the concentrations of permeate were analyzed using UV-spectroscopy (Shimadzu UV-1800) when steady permeate flux was reached during the filtration process.

Measurements were carried out with dextran standards with average molecular weights of 6, 10, 20, 40, and 70 kDa. The test solutions were prepared by dissolving pre-weighed amounts of dextran in DI water. The rejection was calculated based on $R = (C_f - C_p) / C_p$ (where C_p and C_f are the concentrations of permeate and feed solutions, respectively). Details of operating conditions, dextran solution concentrations, characteristic wavelengths and MWCO results are summarized in Table S-1.

Pore size estimation was calculated from MWCO results of dextran as derived from equation (S-1),¹

$$r = 0.33 \times (MWCO)^{0.46} \quad (S-1)$$

where r (Å) is the mean radius of the pore and $MWCO$ (Da) is the molecular weight cutoff at $R = 90\%$.

Table S-1 Molecular weight cutoff determination of pristine TiO₂ membrane and REM

Molecular Weight (kDa)	Characteristic Wavelength (nm)	Initial Concentration C ₀ (wt%)	Rejection (%)		Initial Permeability J ₀ (LMH)	
			TiO ₂	REM	TiO ₂	REM
6	269	0.1	0.1	1.3	626.5	2174.1
10 (9 - 11)	271	0.5	5.2	2.1	617.3	2201.9
20 (15 – 25)	275	0.5	39.2	28.3	630.9	2189.7
40	275	1.0	81.9	77.0	622.0	2165.0
70	275	2.5	95.8	94.2	619.7	2231.4

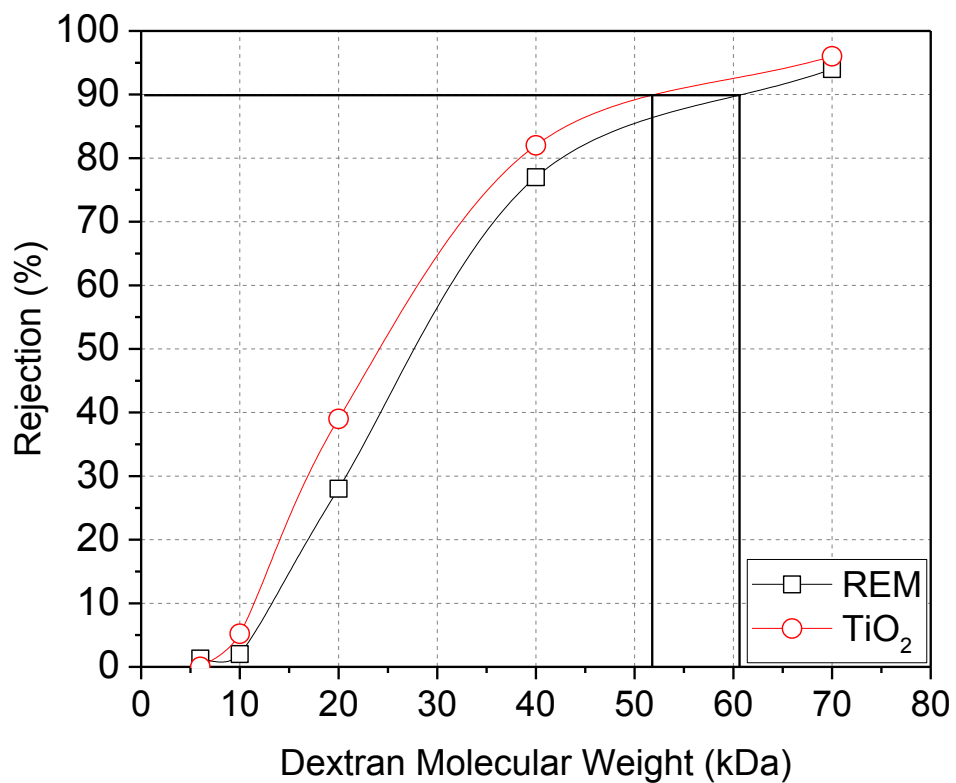


Figure S-2. Molecular weight cutoff determination of a pristine TiO₂ membrane and REM

4) Permeate Flux

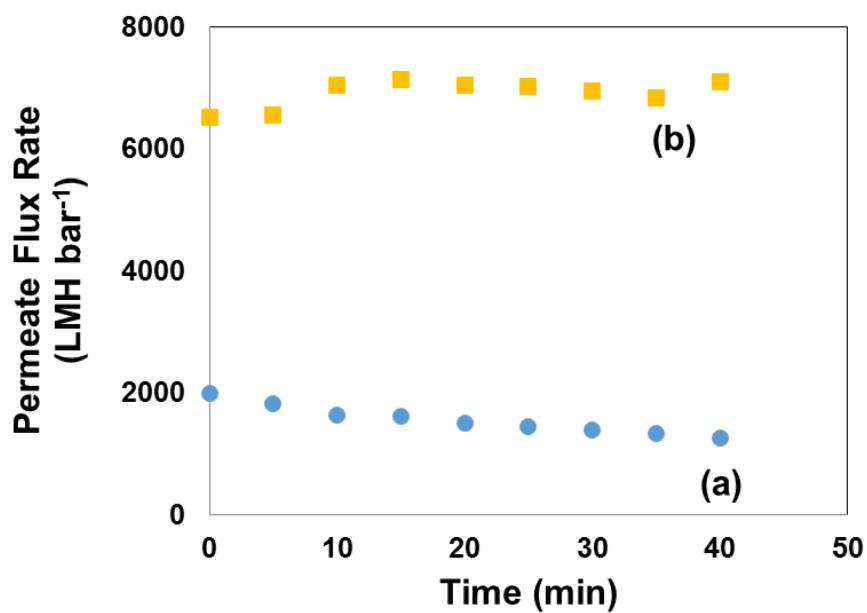


Figure S-3. Pressure-normalized permeate membrane flux profiles for DI water at 21 °C: (a) TiO₂ membrane, and (b) REM-3. Flux rate was tested at $\Delta P = 68.9$ kPa and 50 L h⁻¹ cross flow rate.

5) EIS measurement of electroactive surface area

Electroactive surface area of REM-3 was determined by EIS measurements at the OCP (~ 160 mV), amplitude of ± 4 mV, and a frequency range of 0.01 to 3×10^4 Hz. Experiments were performing in cross-flow filtration mode with a 100 mM NaClO₄ supporting electrolyte and permeate flux of 803 LMH. A transmission line model (TLM) developed by Jing et al.² was used to fit the EIS data. The TLM is able to decouple the impedances at i distinct membrane locations (i = outer membrane surface, active layer pores, or support layer pores) at the membrane-electrolyte interface. EIS data is used to characterize the electro-active surface area at each location, through calculation of the double layer capacitance (C_{dl}) using equation S-2.³

$$C_{dl,i} = \left(\frac{Y_{0,i}}{[r_s^{-1} + R_{ct,i}^{-1}]^{1-\alpha}} \right)^{\frac{1}{\beta}} \quad (\text{S-2})$$

Where r_s is the solution resistance (ohm), $R_{ct,i}$ is the charge transfer resistance (ohm) of location i ; $Y_{0,i}$ is the capacitance (F), and β (dimensionless) is related to an exponential factor that represents the angle of rotation of a purely capacitive line on the complex plane plots. A value of $60 \mu\text{F cm}^{-2}$ was taken as an estimate of the C_{dl} for a metal oxide,⁴ and was used to calculate the electro-active surface area of REM-3. EIS measurements and TLM fit are shown in Figure S-4.

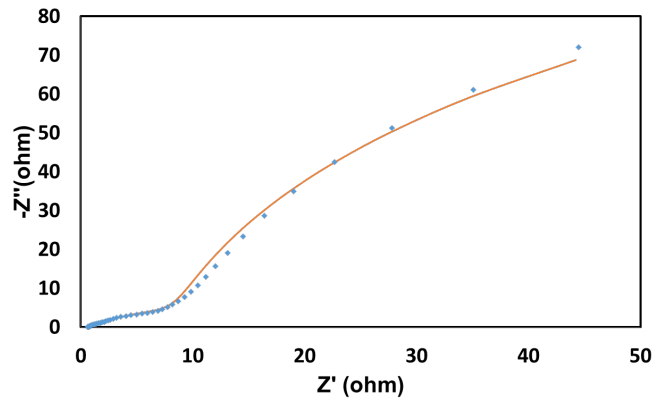


Figure S-4. Measured EIS data for a solution of 5mM Fe(CN)₆⁴⁻ and 5mM Fe(CN)₆³⁻ in 100mM NaClO₄ electrolyte collected at the OCP and T = 21 °C. Solid line is the TLM fit.

6) Oxyanion separation

Nitrate separation experiments were conducted with 1 and 10 mM NaNO₃ solutions. Perchlorate separation experiments were performed with a 9 mM NaClO₄ solution. The REM was polarized as cathode and the stainless rod as anode. Cell potentials from 0 to 10 V were tested. The extended Nernst-Planck equation was used to simulate ClO₄⁻ and NO₃⁻ concentrations in the permeate stream (equation S-3).⁵

$$N_j = J_i C_{p,j} = -D_j \frac{\partial C_{f,j}}{\partial x} - \frac{z_j F}{RT} D_j C_{f,j} \frac{\partial \Phi}{\partial x} + C_{f,j} u \quad (\text{S-3})$$

Where N_j is the molar flux of species j (mol m⁻² s⁻¹); J_i is the membrane permeate water flux (m s⁻¹) calculated at the inner membrane surface; D_j is the diffusion coefficient (m² s⁻¹) (1.32 x 10⁻⁹ for NO₃⁻ and 1.7 x 10⁻⁹ for ClO₄⁻);^{6,7} $C_{p,j}$ and $C_{f,j}$ are the ion concentrations in the permeate and feed solutions, respectively (mol m⁻³); Φ is the applied cell potential (V); u is the average solution velocity in the membrane pore entrance (m s⁻¹); R is the ideal gas constant (J mol⁻¹ K⁻¹); and T is the temperature (294 K). The porosity of the REM was $\theta = 0.304$ (determined by Hg porosimetry analysis), which was applied to estimate u using equation S-4.

$$u = \frac{J}{\theta} \quad (\text{S-4})$$

The flow conditions in the REM reactor allowed diffusion to be ignored ($Pe = 9.85 \times 10^5$), and the electric field is assumed to be linear between the anode and cathode. Therefore, equation S-3 is simplified to the following:

$$C_{p,j} = \frac{C_{f,j} u - \frac{z_j F}{RT} D_j C_{f,j} \frac{\Phi}{L}}{J_i} \quad (\text{S-5})$$

where L is the distance between the anode and cathode (1.7 x 10⁻³ m).

A plot of u versus trans-membrane pressure (ΔP) for REM-3 shows the expected linear trend (Figure S-5). An independent estimate of u using the Hagen-Poiseuille equation was determined

using equation (S-6).

$$u = \frac{r_p^2 \Delta P}{8\eta \Delta x} \quad (\text{S-6})$$

where r_p is the pore radius; η is the fluid viscosity (9.78×10^{-4} Pa s (21 °C)); and Δx is the membrane thickness that ΔP is calculated over. Equation S-6 is used to determine if the ΔP across the membrane is due to the hydraulic resistance of the support layer. For this calculation $\Delta x = 0.5$ cm (entire membrane thickness) and r_p was used to fit equation S-6 to the u measurements (Figure S-5). A fitted value of $r_p = 1.52$ μm was determined, which was nearly identical to the median pore radius of 1.49 μm determined by Hg porosimetry measurements (see manuscript and Section S-1). These results indicate that the ΔP across the membrane is due to the hydraulic resistance of the support layer, and that the effective pore size of the membrane can be determined from fitting r_p to measured flux data.

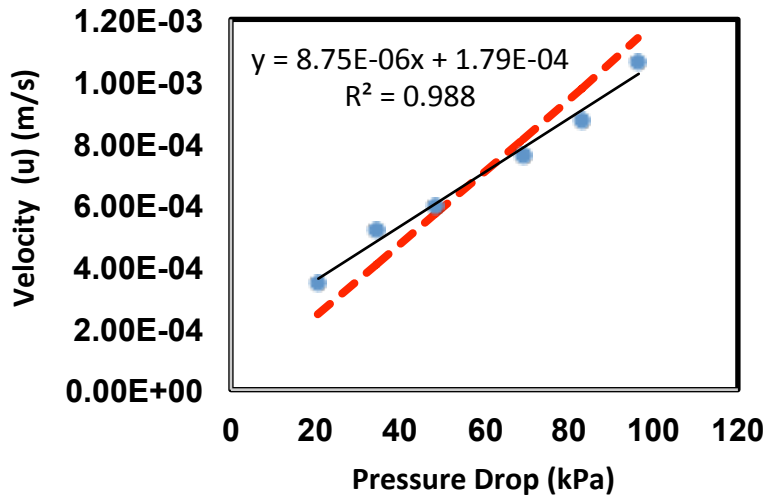


Figure S-5. Comparison of experimental measurements of u versus the pressure drop across the membrane (symbols) to equation S-6 (dashed red line). Solid black line represents linear regression of the experimental data. T = 21 °C.

7) Polarization Curves

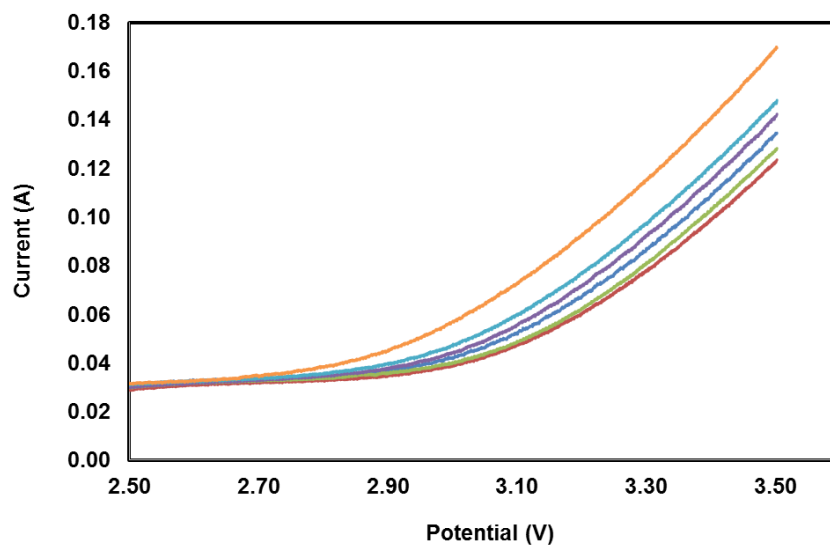


Figure S-6. Polarization curves with 100mM NaClO₄ and at T = 21 °C. From bottom to top, the curves represent polarization profiles for $J = 62, 193, 400, 561, 968,$ and 1243 LMH.

8) Hydroxyl Radical Probe (duplicate experiment)

The following figures show duplicate experiments to those presented in Figure 4 in main text.

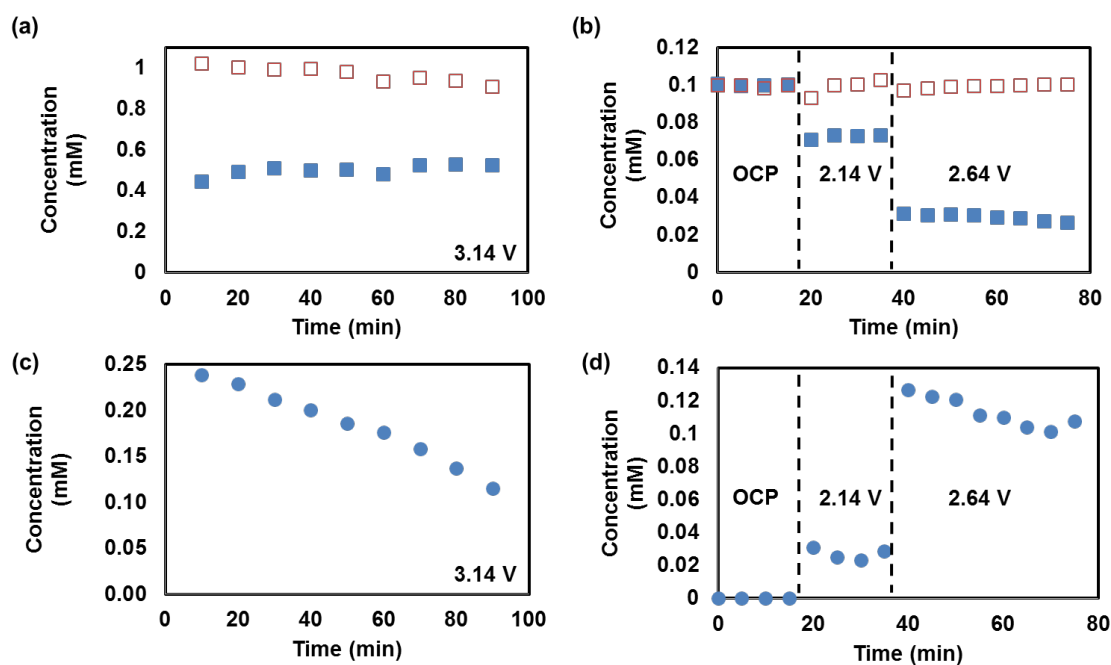


Figure S-7. (a) Concentration profile of COU in the feed and permeate solutions of REM-3 filtration experiment at $J = 132$ LMH. Anodic potential is 3.14V/SHE. (b) The generation of 7-HC during COU oxidation. (c) Concentration profile of TA in the feed and permeate solutions of REM-3. Anodic potential: OCP (0-20 min); 2.14 V (20-40 min); 2.64 V (> 40 min). $J = 110$ LMH. (d) Concentration of HTA during TA oxidation. All experiments were conducted in 100mM NaClO_4 solution and $T = 21^\circ\text{C}$.

9) Energy Consumption Estimation

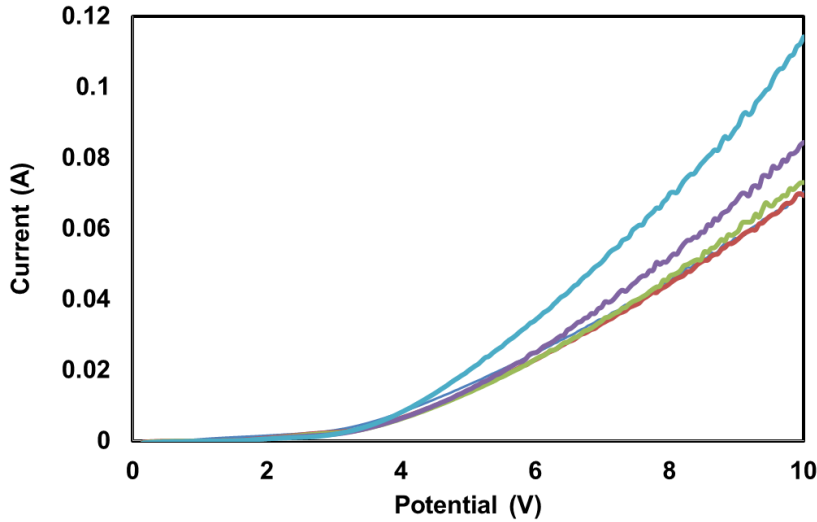


Figure S-8. Polarization curves with 1mM NaNO₃ at 21 °C. From bottom to top, the curves represent polarization profiles for $J = 58, 290, 696, 1006,$ and 1296 LMH. (Curve for $J = 58$ and 290 LMH overlap.)

The energy consumption was calculated based on measured potential and current at a range of J values, and the removal percentage was estimated with the corresponding permeate flux value using Nernst-Plank equation (equation S-5). A solution containing 1mM NO₃⁻ was prepared in 2L DI water without the addition of a supporting electrolyte. Permeate fluxes of $J = 58, 290, 696, 1006$ and 1296 LMH were tested. Under each J value, a linear sweep voltammetry scan was performed from 0 to 10 V. Energy consumption (EC) in kWh m⁻³ was calculated using equation S-7:

$$EC = 2.8 \times 10^{-7} * \frac{VI}{Q} \quad (S-7)$$

where V is potential obtained by LSV (V); I is the corresponding current (A); Q is volumetric flow rate of permeate (m³ s⁻¹); 2.8×10^{-7} is a conversion factor (kW s W⁻¹ h⁻¹).

References

- (1) Aimar, P.; Meireles, M.; Sanchez, V., A contribution to the translation of retention curves into pore size distributions for sieving membranes. *J. Membr. Sci.* **1990**, *54*, 321-338.
- (2) Jing, Y.; Guo, L.; Chaplin, B. P., Electrochemical impedance spectroscopy study of reactive electrochemical membrane fouling and development of a new regeneration scheme. *J. Membr. Sci.* **Under Review**.
- (3) Brug, G. J.; Vandeneeden, A. L. G.; Sluytersrehabach, M.; Sluyters, J. H., The Analysis of electrode impedances complicated by the presence of a constant phase element. *J. Electroanal. Chem.* **1984**, *176*, (1-2), 275-295.
- (4) Levine, S.; Smith, A. L., Theory of differential capacity of oxide-aqueous electrolyte interface. *Discuss. Faraday Soc.* **1971**, (52), 290-301.
- (5) Bard, A. J.; Faulkner, L. R., *Electrochemical Methods: Fundamentals and Applications*. John Wiley & Sons, INC.: 2001.
- (6) Aouina, N.; Cachet, H.; Debiemme-chouvy, C.; Thi, T. M. T., Insight into the electroreduction of nitrate ions at a copper electrode, in neutral solution, after determination of their diffusion coefficient by electrochemical impedance spectroscopy. *Electrochim. Acta.* **2010**, *55*, (24), 7341-7345.
- (7) Heil, S. R.; Holz, M.; Kastner, T. M.; Weingartner, H., Self-diffusion of the perchlorate ion in aqueous-electrolyte solutions measured by Cl-35 Nmr Spin-Echo experiments. *J. Chem. Soc., Faraday Trans.* **1995**, *91*, (12), 1877-1880.